Journal of Alloys and Compounds 520 (2012) 295–300

Contents lists available at SciVerse ScienceDirect

Journal of Alloys and Compounds

journal homepage: www.elsevier.com/locate/jallcom

Microwave absorption properties of in situ grown CNTs/SiC composites

Song Xie[a,b], Guo-Qiang Jin[a], Shuai Meng[a], Yun-Wei Wang[a], Yong Qin[a], Xiang-Yun Guo[a,*]

[a] State Key Laboratory of Coal Conversion, Institute of Coal Chemistry, Taiyuan 030001, PR China
[b] Graduate University of the Chinese Academy of Sciences, Beijing 100039, PR China

ARTICLE INFO

Article history:
Received 10 November 2011
Received in revised form 9 January 2012
Accepted 9 January 2012
Available online 15 January 2012

Keywords:
Absorber
Carbon nanotubes
Permittivity
Permeability
Silicon carbide

ABSTRACT

CNTs/SiC composites were synthesized by pyrolysis of methane over SiC supported nickel catalysts. The composites show good microwave absorption ability in the frequency range of 2–18 GHz. The pyrolysis temperature has profound influences on the microwave absorption characteristic, and 700 °C is the most suitable temperature for preparation of the composites. The microwave absorption characteristic is also influenced by the Ni loading. By varying the Ni loading from 5 wt.% to 7.5 wt.%, the bandwidth of reflection loss below −10 dB can be broadened by 1.5 GHz under the same conditions. For the composite obtained from 7.5 wt.% Ni loading and the pyrolysis temperature of 700 °C, a minimum reflection loss of −37.6 dB can be obtained at 14.5 GHz with a thickness of 1.9 mm and the bandwidth of reflection loss below −10 dB can reach 5.1 GHz (from 12.4 to 17.5 GHz) with a thickness of 2 mm.

1. Introduction

Due to extensive application requirements in electromagnetic interference shielding, microwave absorbing materials (MAMs) have been widely studied in recent years [1–4]. Especially, the studies about microwave absorption properties of ferrites and magnetic metal particles have achieved great progress [5,6]. However, these materials usually have large density and are susceptible to corrosion. Moreover, ferrites and magnetic metals are apt to decrease magnetic loss over GHz due to Snoek's limit, and eddy current and skin depth, respectively [5–9]. These factors restrict the extensive applications of these materials.

Carbon nanotubes (CNTs), known for their unique structure, and excellent electrical, thermal and mechanical properties, have been extensively studied in many fields such as hydrogen storage [10], ceramic reinforcement [11], electrodes [12], and sensors [13]. As MAMs, they also perform well for their excellent dielectric loss ability. CNTs with a helical shape [14], CNTs filled with Fe [15], Co [16], or Ni [17], and CNTs-polymer composites [18,19], have been reported to have great potentials as MAMs.

SiC is a kind of semiconductor materials. It has good thermal conductivity and stability, chemical stability, mechanical strength, and adjustable electrical conductivity. These properties make it a good candidate for MAMs. To be an efficient absorbent, however, it must be surface-modified, composited, or doped with other materials [20–24]. As electrically conductive materials, CNTs usually have relatively large real and imaginary parts of permittivity, which are difficult to match with the complex permeability [14,25–27]. The semiconductor property of SiC could help to tailor the complex permittivity of CNTs, and therefore be suitable to match the complex permeability with a low magnetic metal content.

In this work, SiC supported nickel catalyst was employed to grow CNTs by pyrolysis of methane to produce in situ CNTs/SiC composites with enhanced microwave absorption ability. The unique physicochemical properties of SiC and CNTs enable the composites to be very promising as MAMs, especially for application in severe environments.

2. Experimental

2.1. Materials preparation

The SiC used in this work was prepared by a sol-gel method [28]. Its specific surface area is 35 $m^2\ g^{-1}$. Typically, a certain amount of SiC powder was dispersed into a 1 wt.% $Ni(NO_3)_2$ solution under magnetic stirring. The mass ratio of nickel to SiC in the final mixture was in the range of 5–7.5:100. After 12 h stirring, the solution was dried in a drying oven at 100 °C for 10 h, and then calcined in a muffle furnace at 500 °C for 4 h. To grow CNTs, the obtained NiO/SiC catalyst was placed in a quartz tube and heated to 700 °C at a rate of 5 °C min^{-1}, under a methane flow of 40 sccm. The growth time for all samples was 1 h.

2.2. Materials characterization

The crystalline structures of the samples were characterized by X-Ray diffraction (XRD) with Cu Kα radiation (Model D/max-RB, Rigaku, Japan). The morphologies of the composites were observed by field emission scanning electron microscope (FE-SEM, Model S-4800, Japan) operating at a accelerating voltage of 10 kV, and by a high-resolution transmission electron microscope (HRTEM, Model JEM-2100, Japan) operating at accelerating voltage of 200 kV. Raman spectrum was analysed on a Renishaw Invia micro-Raman spectrometer. Thermogravimetric (TG) results were

* Corresponding author. Tel.: +86 351 4065282; fax: +86 351 4050320.
E-mail address: xyguo@sxicc.ac.cn (X.-Y. Guo).

0925-8388/$ – see front matter © 2012 Elsevier B.V. All rights reserved.
doi:10.1016/j.jallcom.2012.01.050

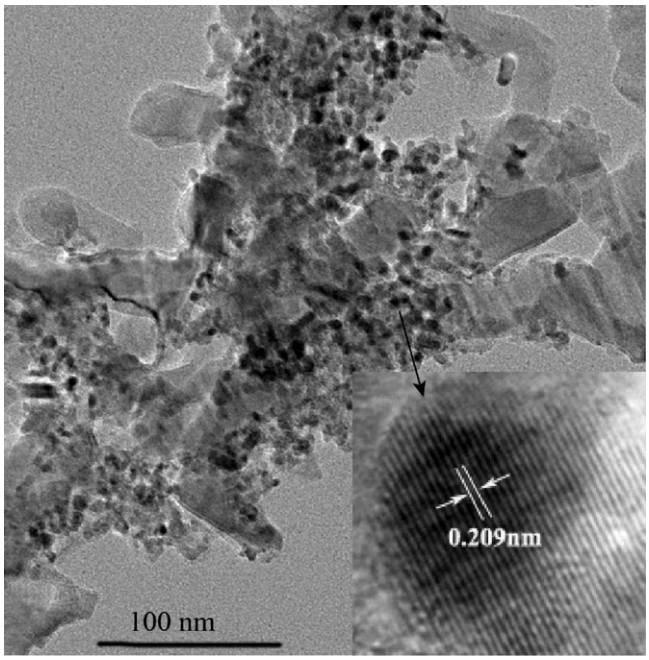

Fig. 1. HRTEM images of 7.5 wt.% Ni/SiC catalyst.

obtained by a thermal analysis system (Model STA 409 PC, Netzsch, Germany) using ca. 5.0 mg of samples and a heating rate of 10 °C min^{-1} in air. The complex permittivity and permeability of the composites were measured by a coaxial line method in the range of 2–18 GHz with a vector network analyzer (Agilent N5230A, USA). The samples were mixed with paraffin (80 wt.%) and pressed into a toroidal shape with an external diameter of 7 mm, an internal diameter of 3 mm, and a thickness of 2 mm.

3. Results and discussion

Fig. 1 shows the HRTEM images of NiO/SiC catalysts. From Fig. 1, it can be seen that the diameter of metallic nanoparticles ranges from 5 to 15 nm, and the lattice spacing of the nanoparticle is 0.209 nm, which corresponds to the NiO (2 0 0) crystal plane. Fig. 2 shows the HRTEM images of the CNTs/SiC composites prepared at the pyrolysis temperature of 700 °C. As seen from Fig. 2, the CNTs have an inner diameter ranging from 5 to 20 nm and an outer diameter ranging from 20 to 50 nm. These CNTs are grown on SiC by the connection of nickel particles (Fig. 2b). Fig. 3 shows FE-SEM image of the CNTs/SiC composite. It can be seen from Fig. 3 that the

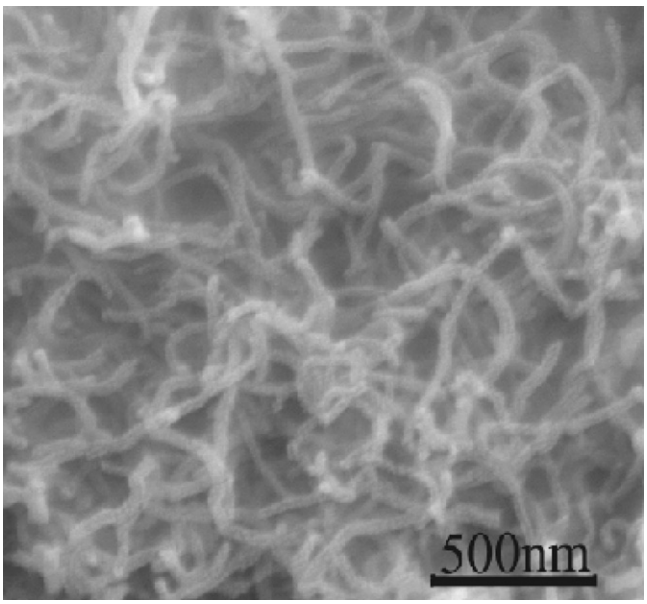

Fig. 3. FE-SEM image of the CNTs/SiC composite prepared from 7.5 wt.% Ni/SiC at 700 °C.

surface of SiC is covered by CNTs. Fig. 4 shows the XRD patterns of the CNTs/SiC composites obtained from different pyrolysis temperatures. The main diffraction peaks can be assigned to graphite and β-SiC. The existence of the graphite peak indicates that the CNTs are graphitic. There are also characteristic peaks of nickel, which result from the reduction of nickel oxide by methane. However, the nickel peaks are relatively weak because of the relatively low content of nickel.

The graphite properties of the composites are further confirmed by Raman analysis. The Raman spectra (Fig. 5) of the composites exhibit two main peaks, which are characteristic peaks of carbon atom bonding state. The D (disordered carbon) band around 1350 cm^{-1} is a breathing mode of A_{1g} symmetry involving phonons near the K zone boundary. This mode is forbidden in perfect graphite and only become active in the presence of disordered carbon. The G (graphitized carbon) band around 1590 cm^{-1} is assigned to zone center phonons of E_{2g} symmetry. This mode results from the stretching vibrations of sp^2 carbon atoms. In general, the intensity ratio of D to G peaks is used to evaluate the crystallinity of carbon [29,30]. From Fig. 5, it can be seen that the value of I_D/I_G

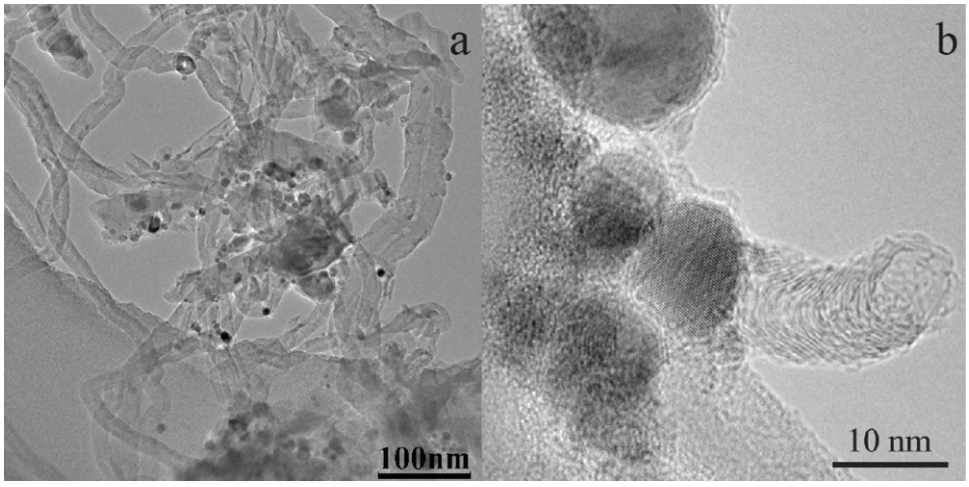

Fig. 2. HRTEM images of the CNTs/SiC composite prepared from 7.5 wt.% Ni/SiC at 700 °C.

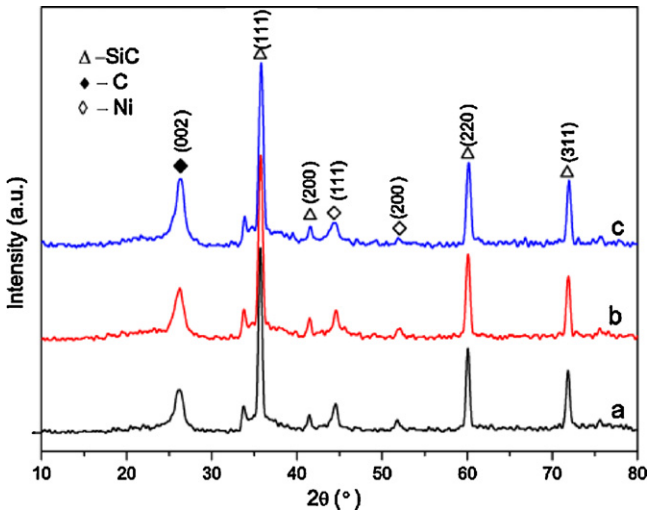

Fig. 4. XRD patterns of CNTs/SiC composites prepared from 7.5 wt.% Ni/SiC at different pyrolysis temperatures: (a) 600 °C, (b) 700 °C, and (c) 800 °C.

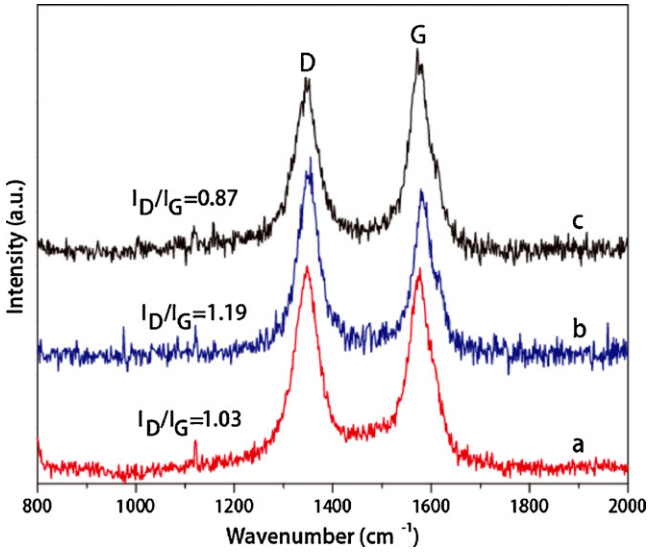

Fig. 5. Raman spectra of CNTs/SiC composites prepared from 7.5 wt.% Ni/SiC and different pyrolysis temperatures: (a) 600 °C, (b) 700 °C, and (c) 800 °C.

is the smallest for the sample prepared at the pyrolysis temperature of 800 °C. In other words, the crystallinity of carbon in the sample is the best, and this is also in agreement with the XRD results.

Fig. 6 shows the TG curves of the composites. As the pyrolysis temperature increases, the relative content of carbon increases, too. In addition, the burning temperature of the composites also increases with the pyrolysis temperature, indicating that the crystallinity of carbon becomes better to some extent. This is consistent with the XRD and Raman results. According to the original ratio of the catalysts and the TG results, the relative contents of SiC, Ni and CNTs are calculated and showed in Table 1.

Table 1
The constituent of different CNTs/SiC composites.

Composite	Ni/SiC-600 °C	Ni/SiC-700 °C	Ni/SiC-800 °C
Mass ratio (SiC:C:Ni)	1:0.46:0.075	1:0.53:0.075	1:0.77:0.075

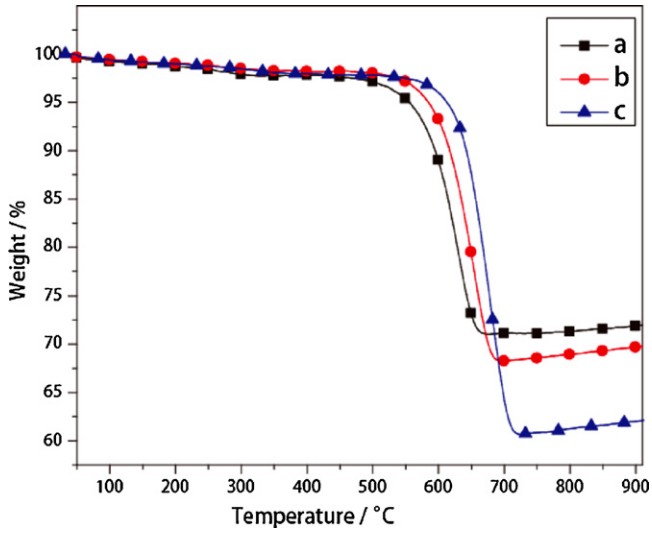

Fig. 6. TG results of CNTs/SiC composites prepared from 7.5 wt.% Ni/SiC and different pyrolysis temperatures: (a) 600 °C, (b) 700 °C, and (c) 800 °C.

According to the transmission line theory, the reflection loss (RL) of the composites can be calculated by the following equations [31,32].

$$\mathrm{RL(dB)} = 20 \lg \left| \frac{Z_{\mathrm{in}} - 1}{Z_{\mathrm{in}} + 1} \right| \quad (1)$$

$$Z_{\mathrm{in}} = \sqrt{\frac{\varepsilon_\gamma}{\mu_\gamma}} \tan h \left[\left(\frac{2\pi f d j}{c} \right) \times \sqrt{\varepsilon_\gamma \mu_\gamma} \right] \quad (2)$$

where Z_{in} is the normalized input impedance in free space, d the thickness of the absorber, c the velocity of light, f the frequency of the electromagnetic wave, $\varepsilon_\gamma = \varepsilon' - j\varepsilon''$ the complex relative permittivity and $\mu_\gamma = \mu' - j\mu''$ the permeability of the material.

Fig. 7 shows the frequency dependence of RL of the composites obtained from different Ni loadings and pyrolysis temperatures. The match thicknesses of all samples are 2 mm. It can be seen from Fig. 7a that the CNTs/SiC composites prepared at the pyrolysis temperature of 700 °C exhibit better absorption ability in the frequency range of 2–18 GHz than the pure SiC. The absorption ability of the composite obtained from 7.5 wt.% Ni is better than that from 5 wt.% Ni. It can also be seen from Fig. 7a, the bandwidth of RL below −10 dB can reach 5.1 GHz (from 12.4 to 17.5 GHz), which is 1.5 GHz broader than that of 5 wt.% Ni loading under the same conditions. Moreover, the absorption peak shifts towards low frequency with the increase of Ni loading. From Fig. 7b, it can be observed that the composites prepared from the pyrolysis temperatures of 600 °C and 800 °C show lower absorption ability than that from 700 °C. These results suggest that the pyrolysis temperature has profound influence on the microwave absorption ability of the composites. Similar phenomenon has also been observed for pure carbon [33].

Fig. 8 shows the RL of the composite obtained from 7.5 wt.% Ni loading and pyrolysis temperature of 700 °C, with different match thicknesses. The bandwidth of RL below −5 dB can reach 10 GHz (from 8 GHz to18 GHz) under the thickness of 2.7 mm. A minimum reflection loss of −37.6 dB can be obtained at 14.5 GHz under the thickness of 1.9 mm. Moreover, the absorption band can be tuned by changing the match thickness. For comparison, Table 2 shows the microwave absorption properties of different absorbers reported in previous references and this work.

In order to understand the possible absorption mechanism, the real and imaginary parts of the complex permittivity and permeability of the composites were investigated. The real part (ε') and imaginary part (ε'') of the complex permittivity represent

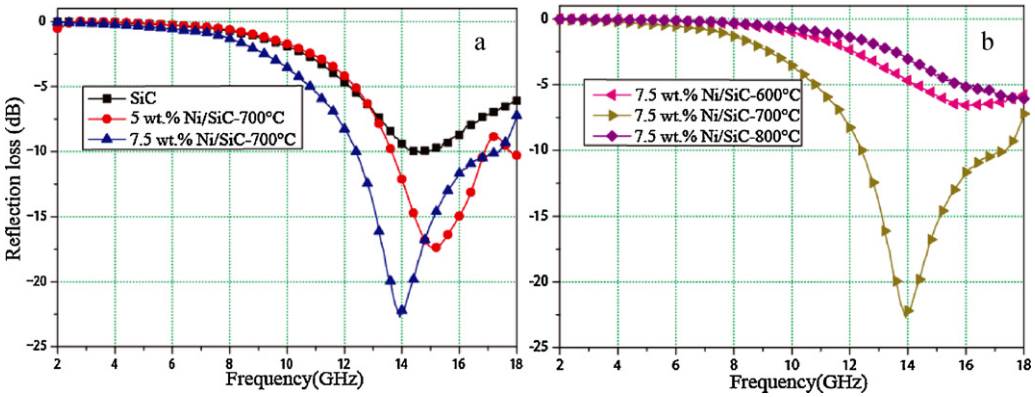

Fig. 7. Frequency dependence of reflection loss of CNTs/SiC composites prepared from different (a) Ni loadings, and (b) pyrolysis temperatures. The match thicknesses of all samples are 2 mm.

Table 2
Microwave absorption properties of different absorbers in literature and this work.

Absorbers	Thickness (mm)	Minimum RL and frequency	Bandwidth over −10 dB (GHz)	Ref.
Fe-filled CNTs	3.5	−22.7 dB at 15.6 GHz	13.1–17.3	[15]
Co-filled CNTs	6.0	−10.1 dB at 2.1 GHz	2.1–2.2	[16]
Ni-filled CNTs	4.0	−23.1 dB at 8.0 GHz	6.4–11	[17]
Co–P-coated SiC	2.3	−32.0 dB at 6.3 GHz	5.8–8.1	[7]
SiC nanowires	2.0	−31.7 dB at 8.3 GHz	7.1–9.6	[23]
CNTs/T-ZnO/EP	2.2	−23.2 dB at 12.8 GHz	10.9–15.3	[25]
CNTs/SiC	1.9	−37.6 dB at 14.5 GHz	12.4–17.5	This work

the energy storage and dissipation capability, respectively. The permittivity loss mainly includes damping loss (arising from the polarization) and ohmic loss (arising from free charge carriers such as electrons in conductors, electrons and holes in semiconductors, and ions in electrolytes) [33]. Both the effect of damping and ohmic losses are included in the imaginary part of the complex permittivity, $\varepsilon'' \approx 1/(2\pi\rho\varepsilon_0 f)$, where ρ is the resistivity [5,34].

From Fig. 9a, it can be seen that the ε' curve of each sample exhibits a decrease from 2 to 18 GHz, with some fluctuations in the range of 6–18 GHz. Meanwhile, the ε'' curve (From Fig. 9b) exhibits an increase along with the frequency. Especially, the ε'' curves of the composites obtained from pyrolysis temperature of 700 °C, exhibit obvious peaks around 16 GHz, suggesting the occurrence of strong resonance. The dielectric tangent loss ($\tan\delta_\varepsilon = \varepsilon''/\varepsilon'$) of this composite is shown in Fig. 10. The $\tan\delta_\varepsilon$ values larger than 0.25 distribute from 12.5 to 18 GHz, indicating that the main dielectric loss occurs in high frequency ranges. In terms of electromagnetic theory such high dielectric loss should result from the intrinsic physical property and structure of the CNTs/SiC composite [35]. From Fig. 9b, the CNTs/SiC composite, obtained from 7.5 wt.% Ni loading and pyrolysis temperature of 700 °C, has a higher ε'' value than others, indicating that the composite has the highest electrical conductivity. This also suggests that the pyrolysis temperature has significant influence on complex permittivity of the composites. Meanwhile, the Raman results (Fig. 5) show that the composite has the highest I_D/I_G, which means that it has relatively more disordered carbon, rather than crystalline carbon. The disordered carbon has more defects and dangling bonds, which can increase the interface scattering and induce the polarization at high frequency. The disordered carbon is also helpful to the formation of conductive networks. These factors then cause a current loss and energy dissipation that both help to increase the dielectric loss. In addition, the interfacial polarization and the associated relaxation occurred at the interfaces among SiC, Ni and CNTs also help to increase the dielectric loss.

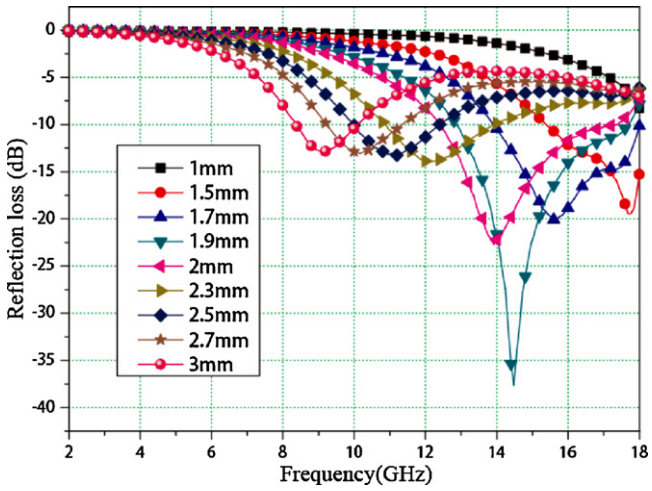

Fig. 8. Reflection loss of the composite prepared from 7.5 wt.% Ni/SiC at 700 °C, with different match thicknesses.

The measured real and imaginary parts of permeability (μ' and μ'') are shown in Fig. 9c and d, respectively. It can be seen that μ' and μ'' of the samples are almost constant, 1 and 0, respectively, due to the relatively low content of nickel. The composites obtained from 700 °C, however, have relatively larger μ' and μ''. This suggests that the pyrolysis temperature of methane also has influence on the complex permeability of the composites.

In general, the magnetic loss of magnetic materials originates mainly from magnetic hysteresis loss, domain wall resonance, eddy current effect, natural resonance and exchange resonance. However, the natural resonance and exchange resonance are the main magnetic loss factors when the frequency is up to GHz. According to Aharoni's theory [36], the exchange resonance occurs at a higher resonance frequency than natural resonance. This prediction is proved in carbon-coated Ni nanocapsules [5], MCNTs filled with Co nanoparticles [16], and carbon–silica–Fe nanocomposites [37]. Therefore, it can be seen from Fig. 9c, the small resonance peak around 5 GHz can be attributed to natural resonance, and the

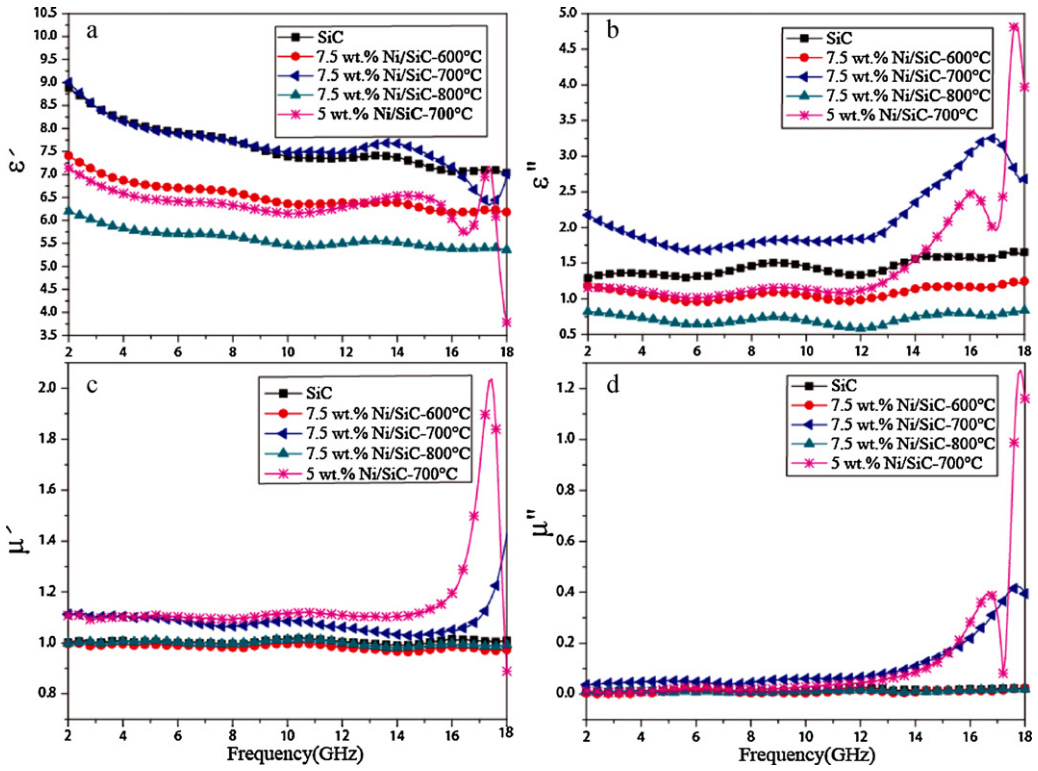

Fig. 9. The measured real (ε') and imaginary (ε'') parts of the complex permittivity and the real (μ') and imaginary (μ'') parts of the complex permeability of CNTs/SiC composites.

other two resonance peaks (around 10 GHz and 17 GHz) can be attributed to exchange resonance. The effect of natural resonance is relatively low in these composites. Both μ'' and ε'' begin to increase near 12 GHz for the composites obtained from 700 °C. This indicates that the increased ε'' accompanies with the increase of μ''. Similar behavior has also been observed in carbon–silica–Fe nanocomposites [37], and CNTs/carbonyl iron [38]. Possibly, the defects and the dangling bonds of carbon, and the interfaces among SiC, Ni and CNTs help to enhance the exchange resonance. Furthermore, the formation of conductive networks increases the electrical conductivity and simultaneously induces a magnetic field, which contributes to magnetic loss. Indeed, it can be seen from Fig. 10 (the tangent loss of 7.5 wt.% Ni/SiC-700 °C sample), the microwave attenuation of this composite results mainly from dielectric loss rather than magnetic loss.

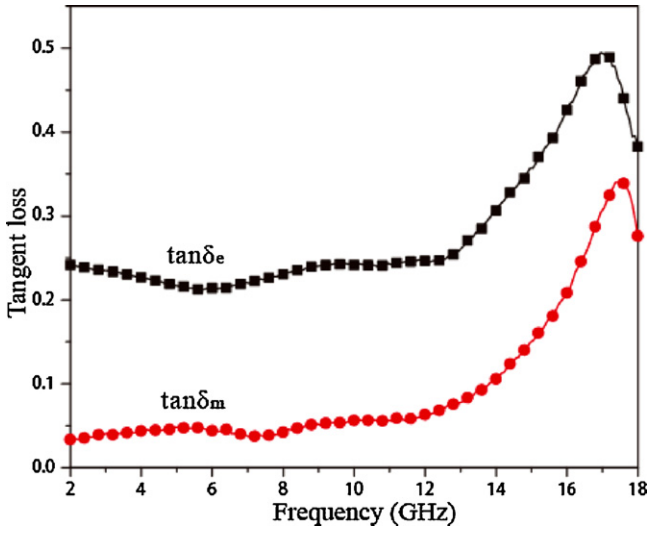

Fig. 10. The tangent loss of the composite prepared from 7.5 wt.% Ni/SiC at 700 °C.

4. Conclusions

A new kind of CNTs/SiC microwave absorber has been prepared by pyrolysis of methane on Ni-loaded SiC. The CNTs/SiC composites exhibit good microwave absorption ability in the frequency range of 2–18 GHz. For the composite obtained from 7.5 wt.% Ni loading and pyrolysis temperature of 700 °C, a minimum RL of −37.6 dB can be obtained at 14.5 GHz under the thickness of 1.9 mm and the bandwidth of RL below −10 dB can reach 5.1 GHz (from 12.4 to 17.5 GHz) under the thickness of 2 mm. The RL comes from both dielectric loss and magnetic loss, but the former contributes more. Through the combination of SiC and CNTs, the materials exhibit a suitable complex permittivity to match the complex permeability with a low magnetic metal content. The composites are lightweight, corrosion-resistant, mechanically strong and thermostable candidate for microwave absorption.

Acknowledgement

This work was financially supported by the Institute of Coal Chemistry, Chinese Academy of Sciences (Ref. 2011SQZBJ14).

References

[1] M. Itoh, M. Terada, F. Shogano, K.I. Machida, J. Appl. Phys. 108 (2010) 0639111–0639115.
[2] R.T. Ma, H.T. Zhao, G. Zhang, Mater. Res. Bull. 45 (2010) 1064–1068.
[3] N.J. Tang, W. Zhong, C.T. Au, Y. Yang, M.G. Han, K.J. Lin, Y.W. Du, Synthesis, J. Phys. Chem. C 112 (2008) 19316–19323.
[4] C.W. Qiang, J.C. Xu, Z.Q. Zhang, L.L. Tian, S.T. Xiao, Y. Liu, P. Xu, J. Alloys Compd. 506 (2010) 93–97.
[5] X.F. Zhang, X.L. Dong, H. Huang, Y.Y. Liu, W.N. Wang, X.G. Zhu, B. Lv, J.P. Lei, C.G. Lee, Appl. Phys. Lett. 89 (2006) 0531151–0531153.

[6] J.R. Liu, M. Itoh, M. Terada, T. Horikawa, K.I. Machida, Appl. Phys. Lett. 91 (2007) 093101–093103.
[7] Y. Li, R. Wang, F. Qi, C. Wang, Appl. Surf. Sci. 254 (2008) 4708–4715.
[8] A. Ghasemi, A. Hossienpour, A. Morisako, X.X. Liu, A. Ashrafizadeh, Mater. Des. 29 (2008) 112–117.
[9] J.H. Zhu, S.Y. Wei, N. Haldolaarachchige, D.P. Young, Z.H. Guo, J. Phys. Chem. C 115 (2011) 15304–15310.
[10] C.H. Chen, C.C. Huang, Microporous Mesoporous Mater. 109 (2008) 549–559.
[11] S.C. Zhang, W.G. Fahrenholtz, G.E. Hilmas, E.J. Yadlowsky, J. Eur. Ceram. Soc. 30 (2010) 1373–1380.
[12] W. Wei, J.L. Wang, L.J. Zhou, J. Yang, B. Schumann, Y.N. NuLi, Electrochem. Commun. 13 (2011) 399–402.
[13] R. Mangu, S. Rajaputra, V.P. Singh, Nanotechnology 22 (2011) 215502–215506.
[14] X.S. Qi, Y. Yang, W. Zhong, Y. Deng, C.T. Au, Y.W. Du, J. Solid State Chem. 182 (2009) 2691–2697.
[15] H.Y. Lin, H. Zhu, H.F. Guo, L.F. Yu, Mater. Lett. 61 (2007) 3547–3550.
[16] H.B. Yi, F.S. Wen, L. Qiao, F.S. Li, J. Appl. Phys. 106 (2009) 1039221–1039224.
[17] T.C. Zou, H.P. Li, N.Q. Zhao, C.S. Shi, J. Alloys Compd. 496 (2010) L22–L24.
[18] D. Makeiff, T. Huber, Synth. Met. 156 (2006) 497–505.
[19] Y.C. Qing, W.C. Zhou, F. Luo, D.M. Zhu, Carbon 48 (2010) 4074–4080.
[20] Z.Y. Chu, H.F. Cheng, Y.J. Zhou, Q. Wang, J. Wang, Mater. Des. 31 (2010) 3140–3145.
[21] H.J. Zhang, X.W. Wu, Q.L. Jia, X.L. Jia, Mater. Des. 28 (2007) 1369–1373.
[22] D.L. Zhao, F. Luo, W.C. Zhou, J. Alloys Compd. 490 (2010) 190–194.
[23] S.C. Chiu, H.C. Yu, Y.Y. Li, J. Phys. Chem. C 114 (2010) 1947–1952.
[24] H.L. Zhu, Y.J. Bai, R. Liu, N. Lun, Y.X. Qi, F.D. Han, J.Q. Bi, J. Mater. C 21 (2011) 13581–13587.
[25] H.F. Li, J. Wang, Y.H. Huang, X.Q. Yan, J.J. Qi, J. Liu, Y. Zhang, Mater. Sci. Eng. B-Adv. Funct. Solid State Mater. 175 (2010) 81–85.
[26] D.L. Zhao, X. Li, Z.M. Shen, J. Alloys Compd. 471 (2009) 457–460.
[27] D.L. Zhao, J.M. Zhang, X. Li, Z.M. Shen, J. Alloys Compd. 505 (2010) 712–716.
[28] G.Q. Jin, X.Y. Guo, Microporous Mesoporous Mater. 60 (2003) 207–212.
[29] A.C. Ferrari, J. Robertson, Phys. Rev. B 61 (2000) 14095–14107.
[30] F. Tuinstra, J.L. Koenig, J. Chem. Phys. 53 (1970) 1126–1130.
[31] Q.M. Su, J. Li, G. Zhong, G.H. Du, B.S. Xu, J. Phys. Chem. C 115 (2011) 1838–1842.
[32] R.C. Che, L.M. Peng, X.F. Duan, Q. Chen, X.L. Liang, Adv. Mater. 16 (2004) 401–404.
[33] Y.C. Du, J.Y. Wang, C.K. Cui, X.R. Liu, X.H. Wang, X.J. Han, Synth. Met. 160 (2010) 2191–2196.
[34] D.K. Cheng, Field and Wave Electromagnetics, second ed., Addison-Wesley, New York, 1989.
[35] Y.J. Chen, G. Xiao, T.S. Wang, Q.Y. Ouyang, L.H. Qi, Y. Ma, P. Gao, C.L. Zhu, M.S. Cao, H.B. Jin, J. Phys. Chem. C 115 (2011) 13603–13608.
[36] A. Aharoni, J. Appl. Phys. 69 (1991) 7762–7764.
[37] J.P. He, J.H. Zhou, G.X. Li, T. Wang, D. Sun, X.C. Ding, J.Q. Zhao, S.C. Wu, J. Phys. Chem. C 114 (2010) 7611–7617.
[38] G.X. Tong, W.H. Wu, Q. Hua, Y.Q. Miao, J.G. Guan, H.S. Qian, J. Alloys Compd. 509 (2011) 451–456.